SUPPLEMENTARY INFORMATION

Iteration-Dependence of IBU

Supplementary Figure 1 shows the impact of adding more iterations for IBU to the plot that appeared in Fig. 7. As the number of iterations increases, the oscillation behavior becomes more pronounced. Oscillations are already present with $N = 10$, but are significantly smaller than for other algorithms. Stopping the iterative procedure early is a regularization that can help damp oscillations that are known to become large as $N \to \infty$.

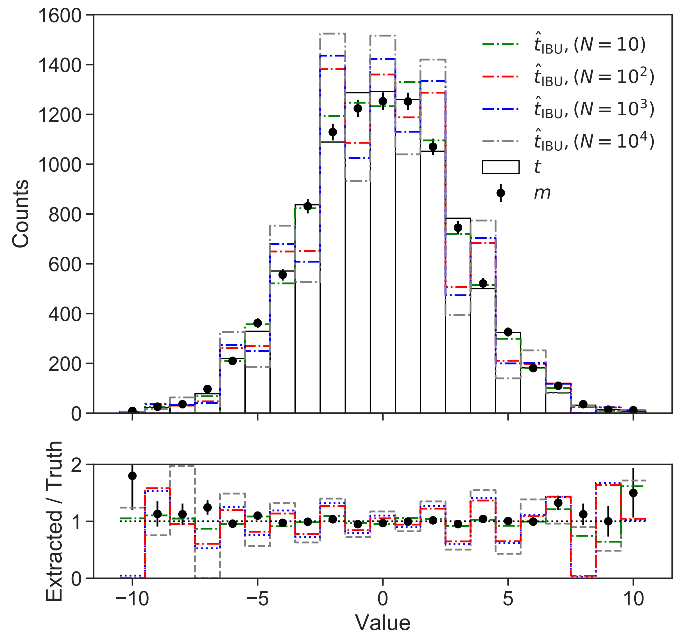

Supplementary Figure 1. The same as Fig. 7, but with increasingly many iterations (N) for IBU.

Alternative Configurations of the IBM Q Johannesburg Machine

The readout errors of a quantum computer depend on its connectivity. The results presented in Fig. 10 used a particular subset of 5 qubits out of the 20 qubits available. Supplementary Figure 2 presents the results for four different configurations, corresponding to taking four rows of the computer qubits. In each row, every qubit is connected to its two neighbors. The first and last qubit in each row is connected to the row above or below. The middle qubits in the middle two rows are additionally connected to each other. Therefore, every qubit in the first and last rows have only two connections while two of the qubits in the middle rows have two connections and the other three qubits have three connections.

Uncertainties when using IBM Q Response Matrix

Supplementary Figures 3 and 4 are the analogs for Fig.5 and 6, but for the example shown in Fig. 9 which is based on an IBM Q response matrix.

Alternative to Harmonic Oscillator Ground State

Supplementary Figure 5 presents a spiky distribution instead of a smooth probability density, as typified by the ground state of the harmonic oscillator. The state corresponds to the W distribution [**?**]: $|W\rangle = \frac{1}{\sqrt{n}}(|100\cdots0\rangle + |010\cdots0\rangle + \cdots |00\cdots01\rangle)$. As the true distribution is exactly zero for most states, the matrix

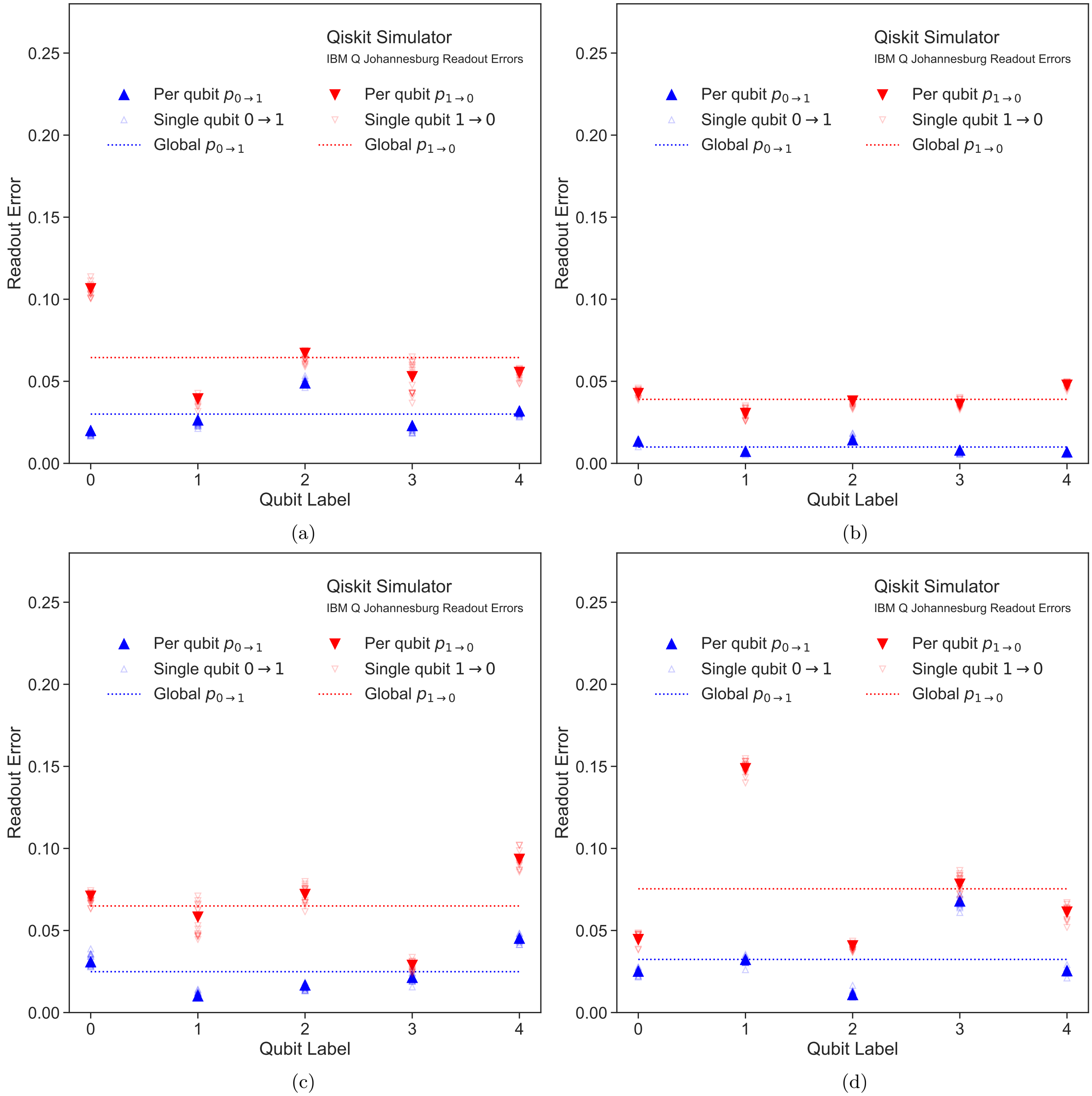

Supplementary Figure 2. The same test of universality as in Fig. 10, using various configurations of the IBM Q Johannesburg machine. From top left, clockwise, the plots correspond to rows 1-4 as described in the text.

inversion has large fluctuations because there is nothing special about zero for this method (can give negative results). In contrast, the `ignis` and IBU methods are always positive and have smaller deviations. Supplementary Figure 6 shows that the mean squared error for IBU is lower than `ignis` for tens of iterations.

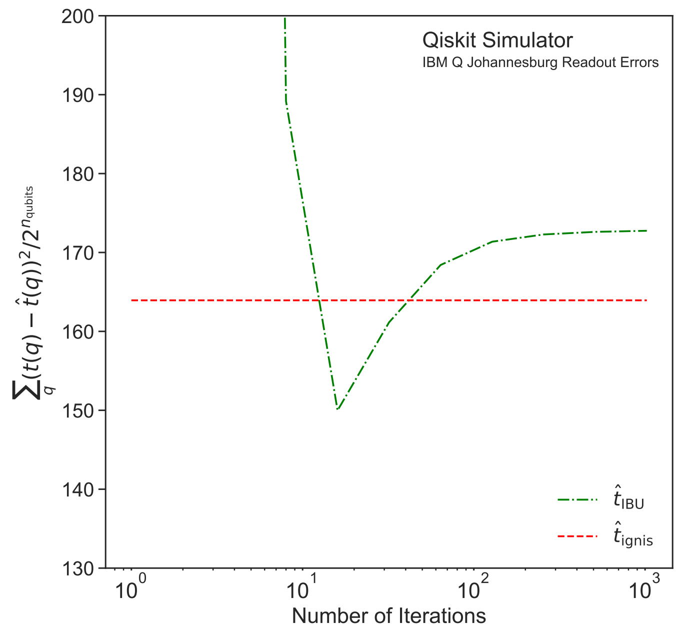

Supplementary Figure 3. The difference between $\hat{t}_{\rm IBU}$ and t as a function of the number of iterations for the example presented in Fig. 5. By definition, the **ignis** method does not depend on the number of iterations.

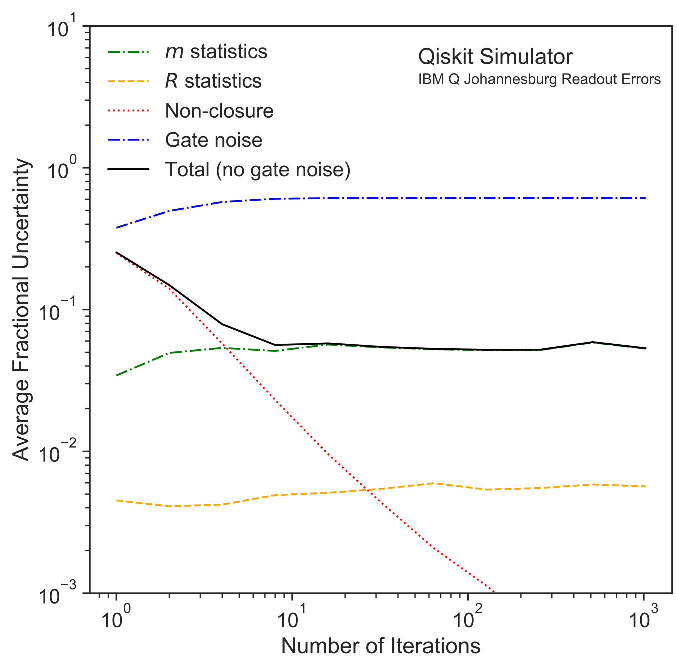

Supplementary Figure 4. Sources of uncertainty for $\hat{t}_{\rm IBU}$ as a function of the number of iterations for the example presented in Fig. 6. Each uncertainty is averaged over all states. The total uncertainty is the sum in quadrature of all the individual sources of uncertainty, except gate noise (which is not used in the measurement simulation, but would be present in practice).

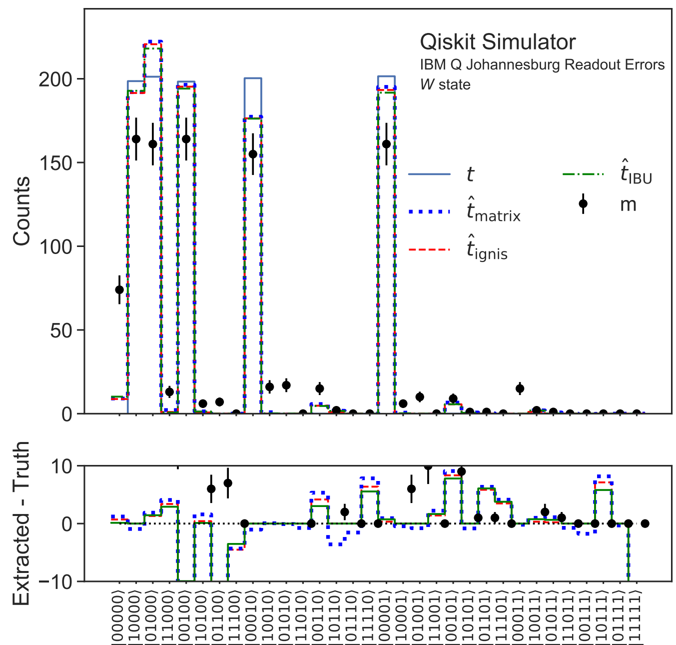

Supplementary Figure 5. The measurement of the noisy W distribution using the response matrix from the IBM Q Johannesburg machine. 1000 shots are used for the state measurement and $500 \times 2^{n_{\text{qubits}}}$ shots are used to construct the response matrix. IBU uses 100 iterations. Note that unlike for Fig. 2 and 3, the true distribution is the theoretical W distribution and not the true pre-readout-noise distribution. This is because the W state is prepared as fully entangled prior to measurement.

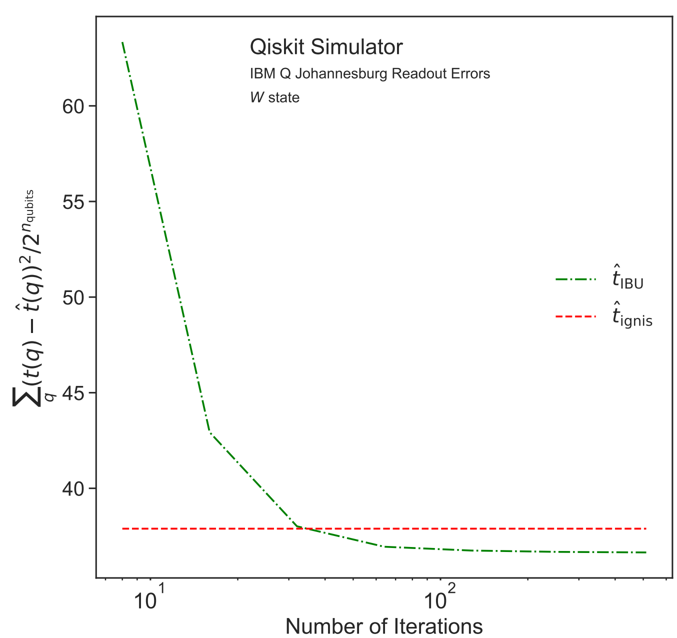

Supplementary Figure 6. The mean squared error between the unfolded and theoretical W state distribution as a function of the number of iterations in the IBU method.